

MODELING HEIGHT PROFILE FOR DROP-ON-DEMAND PRINT OF UV CURABLE INK

Yumeng Wu

School of Mechanical Engineering
Purdue University
West Lafayette, Indiana 47907
Email: wu350@purdue.edu

George Chiu*

School of Mechanical Engineering
Purdue University
West Lafayette, Indiana 47907
Email: gchiu@purdue.edu

ABSTRACT

This paper proposes a height profile model for drop-on-demand printing of UV curable ink. Existing models include superposition of single drops, numerical models, and graphic-based model. They are either too complicated or over simplified. Graphic model intends to find a sweet spot in between, however, accuracy is marginally improved from superposition model while it demands more computation. The proposed model aims to achieve the same as graphic model by introducing volume and area propagation matrices to reflect the localized ink flow from higher location to the lower, while avoiding the detailed physics behind it. This model assumes a constant volume and area propagation of subsequent drop due to height profile difference. It is validated with experiments on single drop, 2-drop and 3-drop line printing. Stability of this model is analyzed. Using root mean square (RMS) error as benchmark, proposed model achieves 6.6% along the center row and 7.4% overall, better than existing models.

NOMENCLATURE

- a_{ij} Area covered by a single drop at (i, j) .
 v_{ij} Drop volume at cell (i, j) .
 h_{ij} Average height of a single drop at cell (i, j) .
 $a_{ij,k}$ Area coverage at cell (i, j) after the k^{th} drop is deposited.
 $v_{ij,k}$ Drop volume at cell (i, j) after the k^{th} drop is deposited.
 $h_{ij,k}$ Average height at cell (i, j) after the k^{th} drop is deposited.

- Δv_{ij} Volume change at cell (i, j) .
 Δa_{ij} Area change at cell (i, j) .
 $A_j[0]$ Area matrix in the new area of interest before additional drop is deposited at cell $(1, j)$.
 $V_j[0]$ Volume matrix in the new area of interest before additional drop is deposited at cell $(1, j)$.
 $A_j[1]$ Area matrix in the new area of interest after additional drop is deposited at cell $(1, j)$.
 $V_j[1]$ Volume matrix in the new area of interest after additional drop is deposited at cell $(1, j)$.
 $H_j[1]$ Height matrix in the new area of interest after additional drop is deposited at cell $(1, j)$.
 d Nominal pitch between two drops.
 r Radius of single drop's footprint on substrate.

1 INTRODUCTION

3D printing, or additive manufacturing (AM), has gained traction in interests and applications. Comparing to traditional subtractive manufacturing, e.g. CNC machining, the benefits of AM include less waste of materials, ability to manufacture more complex geometry and lower cost on small to median batch production [6].

Among different additive manufacturing processes [2], material jetting is unique for its similarity with traditional ink-jet printing. Two fundamental categories of ink-jet printing are continuous jetting and drop-on-demand (DoD) [9]. In DoD inkjet, drops are formed by either squeezing with piezoelectric ink-jet

*Address all correspondence to this author.

or heating with thermal ink-jet. While traditional ink-jet printing can dispense a wide range of materials, from color inks to polymers and nanoparticles [11], material jetting requires inks that can be solidified under prescribed conditions. Among such materials, photosensitive inks, which solidifies under light of certain wavelengths, are commonly used. Commercial printers, such as Acuity EY series from FUJIFILM, HP Scitex FB500, use UV curable inks. Typically, cured drop diameters range from 50 to 500 μm , depending on the nozzle size [4]. With decades of studies on ink-jet printing, many approaches have been proposed to improve print quality [1, 10]. Majority of these approaches focus on color and image quality. Mimaki shows that material jetting is capable of doing additive manufacturing in full color. However, the height resolution is lower than that of color. Adapting optimization on color and image quality to geometry, especially height profile, of products made by material jetting can be effective. Such optimization requires a height profile model to balance between accuracy and computation.

For DoD inkjet print of UV curable ink, a single drop is commonly modeled as a spherical cap [5]. Treating multiple drops as superposition of single drop is commonly applied, but leads to large errors, because many key physical properties are ignored. There are other numerical models considering many parameters [3, 7]. Guo [8] introduced a model for the purpose of control, however, the graph-based dynamic model propagates height directly does not guarantee conservation of volume. Moreover, its root mean square (RMS) errors are often greater than 10%, which is on par with simple superposition model.

In this paper, a height profile model is developed to reflect the physical movement of inks on non-porous surface when the subsequent drop is deposited next to a cured drop. This model calculates height indirectly from volume distribution and area propagation. The remaining of the paper is organized as follow. the height profile model is introduced in Section 3. Propagation model is discussed in Section 3. Experimental validation is included in Section 4. Section 5 is the conclusion.

2 SINGLE DROP HEIGHT PROFILE MODEL

Figure 1 illustrates a single drop height profile model and defines notations. Figure 1.(a) shows 3×3 square cells, where a drop of material can be deposited at the center of each cell. The size of each cell is $d \times d$, where d is the pitch between two adjacent drops. Assuming a single drop deposited on a flat non-porous surface forms a spherical cap with radius r , if $0.5d \leq r < 1.5d$, the drop covers the 3×3 cells, see the shaded area in Fig. 1(a). This range of pitch distance is used to make enough overlap between adjacent drops to ensure print quality. Each cell is indexed by (i, j) , where i is the row index and j is the column index. Both i and j start from 0.

The height profile of a single drop is denoted by a 3×3

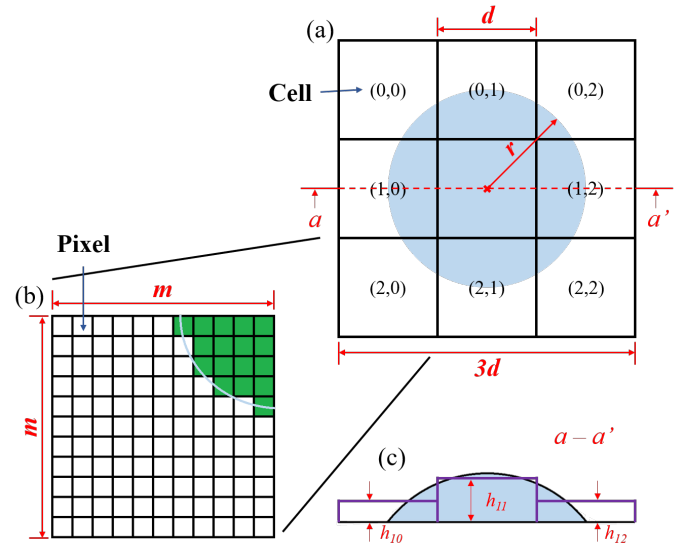


FIGURE 1. (a): Single drop with radius r on 3×3 cell. (b): Zoomed-in section of cell (2,0) in (a), illustrating how to count area covered by inks. (c): Height profile comparison of center row. Proposed height profile is in purple, while spherical cap height profile is in light blue.

matrix,

$$H = \begin{bmatrix} h_{00} & h_{01} & h_{02} \\ h_{10} & h_{11} & h_{12} \\ h_{20} & h_{21} & h_{22} \end{bmatrix}, \quad (1)$$

where h_{ij} denotes the average height of the drop in cell (i, j) , which is computed from the ratio between the drop volume within the cell and the area covered by the drop within the cell covered by the drop. Figure 1.(c) illustrates the height profiles of cells (1,0), (1,1) and (1,2). Area in light blue represents the height profile from the spherical cap model. Horizontal purple lines represent the proposed height profile.

To compute the height profile, a high-resolution optical profilometer is used to measure the drop profile with fine spatial resolution. Figure 1.(b) illustrates the optical profilometer image for cell (2,0) of Fig. 1.(a), where each cell image is represented by $m \times m$ pixels. The area under each pixel (a_c) is $\frac{d^2}{m^2}$. In Fig. 1.(b), the area covered by the drop is shown in green. For each pixel, the height h_{i_m, j_m} is non-zero if it is covered by the drop and is zero if it is not covered by the drop, where $i_m, j_m = 0, \dots, m-1$ are pixel indices within a cell. Assuming M pixels within cell (i, j) are covered by the drop, the area occupied by the drop $a_{ij} = M a_c$. Similar to the height profile, the area covered by a single drop can

be denoted by

$$A = \begin{bmatrix} a_{00} & a_{01} & a_{02} \\ a_{00} & a_{11} & a_{12} \\ a_{00} & a_{21} & a_{22} \end{bmatrix}, \quad (2)$$

where a_{ij} denotes the area covered by the drop in cell (i, j) .

The drop volume within cell (i, j) can be computed by

$$v_{ij} = \sum_{i_m=0}^{m-1} \sum_{j_m=0}^{m-1} h_{i_m j_m} a_c \quad (3)$$

Similarly, the volume of a single drop can be denoted by

$$V = \begin{bmatrix} v_{00} & v_{01} & v_{02} \\ v_{00} & v_{11} & v_{12} \\ v_{00} & v_{21} & v_{22} \end{bmatrix}, \quad (4)$$

where v_{ij} denotes the drop volume within cell (i, j) .

Given a_{ij} and v_{ij} , the average height of cell (i, j) denoted by h_{ij} can be obtained by

$$h_{ij} = \frac{v_{ij}}{a_{ij}} = \frac{\sum_{i_m=0}^{m-1} \sum_{j_m=0}^{m-1} h_{i_m j_m}}{M} \quad (5)$$

Experiments were conducted to obtain the height profile model for a single drop. The experimental setup includes a Microdrop piezo-electrical dispensing system MD-K-140, a XY Stage, a UV light and a Zeta-20 optical profiler. The dispenser head has a heated nozzle tip of $70 \mu\text{m}$. Zeta-20 has a $0.35\times$ coupler with $2/3''$ camera and we used $100\times$ objective lens for all measurements. The Z resolution in this setting is $0.04 \mu\text{m}$.

Microscope slide is chosen as the substrate for its flatness. The dispensing head is mounted on a linear stage. The UV inks (C-Flex 12-050 Black) are obtained from Kao Collins Inc. Its viscosity is 17.2 cP at 22.4°C . In this study, the pitch is set to $70 \mu\text{m}$ and the measured drop radius r is around $140 \mu\text{m}$.

To obtain the height profile for a single drop, 50 drops are deposited on to a glass substrate. For each drop, a_{ij} and v_{ij} are obtained from experimental data and Eq. (3), respectively. The average area and volume covered by a single drop is computed as the average of the 50 samples, see Table 1 and 2, respectively. The height profile is then computed from the ratio between the average volume and the average area coverage, see Table 3. Figure 2.(a) is the height contour of one of the samples. Red lines mark the cell boundaries. Figure 2.(b) compares the measured height along center row of this sample and the average cell height along center row of 50 samples.

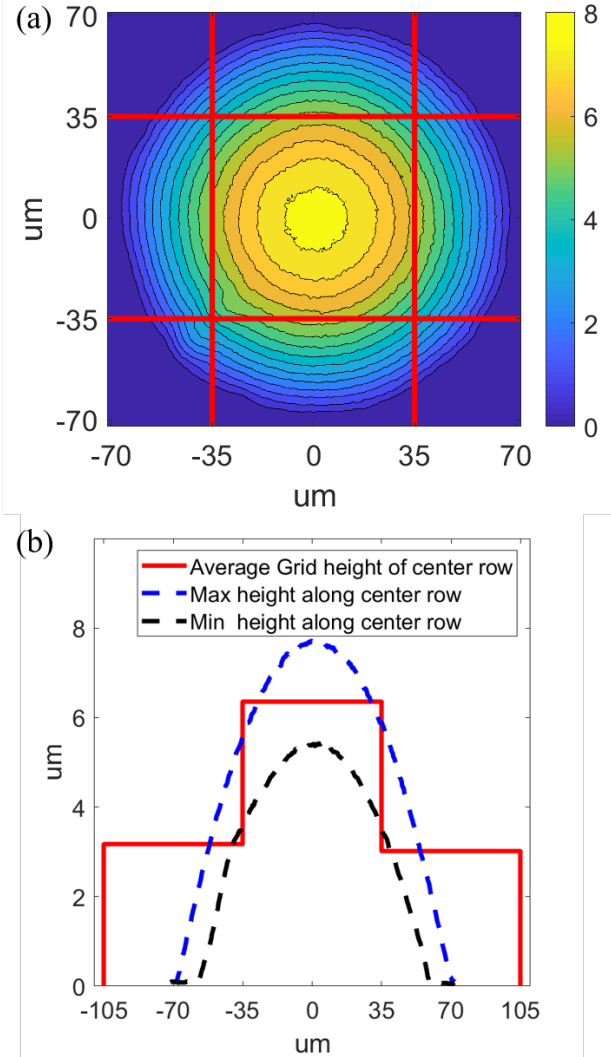


FIGURE 2. (a): contour of single drop, marked with $70 \mu\text{m}$ pitch size. (b): dash lines are height measurements of the sample in a), with blue dash line showing the maximum height along the center row and black dash line showing the minimum height along the center row; red solid line shows the average cell height long center row.

3 HEIGHT PROFILE MODEL FOR MULTIPLE ADJACENT DROPS

We assume non-adjacent drops deposited on non-porous flat surface have the same height profile. When the drop is deposited on non-flat surface, localized ink flow will occur. Such flow depends on many parameters, such as viscosity and surface tension, which requires complicated and detailed material model. To simplify computation, we assume that the average height in each cell changes due to additional ink volume and changes in area cover-

TABLE 1. Volume (μm^3) in each cell for a single drop.

474.52	5480.10	490.56
6105.06	31527.32	6131.28
479.55	5646.20	484.74

TABLE 2. Occupied area (μm^2) in each cell for a single drop.

340.04	1942.06	334.10
1923.37	4961.90	2033.16
338.93	1960.20	333.75

TABLE 3. Average cell height (μm) in each cell for a single drop.

1.40	2.82	1.47
3.17	6.35	3.02
1.41	2.88	1.45

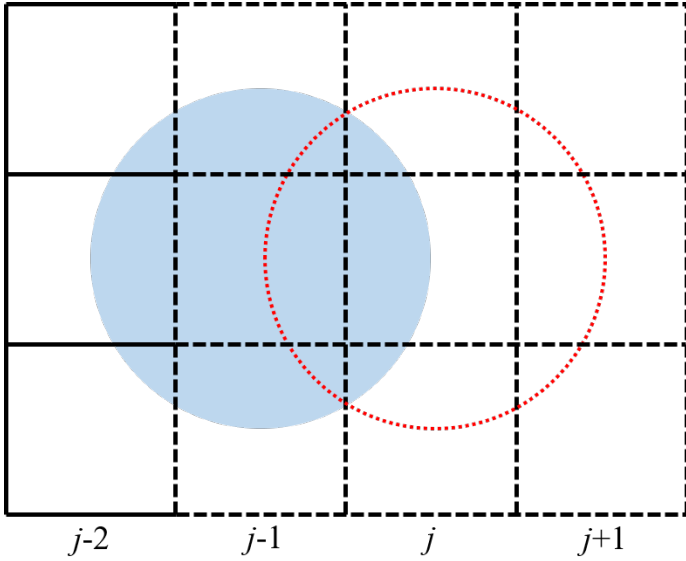


FIGURE 3. Light blue circle represents the $(k-1)^{th}$ drop centered at cell $(1, j-1)$ and red dashed circle represents the k^{th} drop centered at cell $(1, j)$. When the k^{th} drop is deposited, the dashed 3×3 cells are the new area of interest.

age, i.e.

$$h_{ij,k} = \frac{v_{ij,k-1} + \Delta v_{ij}}{a_{ij,k-1} + \Delta a_{ij}}, \quad (6)$$

where $h_{ij,k}$ is the height after the k^{th} drop, $v_{ij,k-1}$ and $a_{ij,k-1}$ are the volume and area before the k^{th} drop, Δv_{ij} and Δa_{ij} are the changes in volume and area due to the additional drop.

Figure 3 illustrates the impact of a new k^{th} drop deposited at cell $(1, j)$, next to a previously deposited $(k-1)^{th}$ drop at cell $(1, j-1)$. The 3×3 dashed cells represent the new area of interest associated with the new drop.

Since there can be either 0 or 1 drop in a single cell, we extend the height profile matrix H notation in Eq. (1) to accommodate for this. The height profile of the new area of interest centered at cell $(1, j)$ is given by

$$H_j[0] = \begin{bmatrix} h_{0j-1,k-1} & h_{0j,k-1} & 0 \\ h_{1j-1,k-1} & h_{1j,k-1} & 0 \\ h_{2j-1,k-1} & h_{2j,k-1} & 0 \end{bmatrix}, H_j[1] = \begin{bmatrix} h_{0j-1,k} & h_{0j,k} & h_{0j+1,k} \\ h_{1j-1,k} & h_{1j,k} & h_{1j+1,k} \\ h_{2j-1,k} & h_{2j,k} & h_{2j+1,k} \end{bmatrix}, \quad (7)$$

where $H_j[0]$ represents the height profile of the new area of interest before the k^{th} drop has been deposited at cell $(1, j)$; $H_j[1]$ represents the height profile of the new area of interest after the k^{th} drop has been deposited at cell $(1, j)$.

Similarly, The drop volume of the new area of interest centered at cell $(1, j)$ is given by

$$V_j[0] = \begin{bmatrix} v_{0j-1,k-1} & v_{0j,k-1} & 0 \\ v_{1j-1,k-1} & v_{1j,k-1} & 0 \\ v_{2j-1,k-1} & v_{2j,k-1} & 0 \end{bmatrix}, V_j[1] = \begin{bmatrix} v_{0j-1,k} & v_{0j,k} & v_{0j+1,k} \\ v_{1j-1,k} & v_{1j,k} & v_{1j+1,k} \\ v_{2j-1,k} & v_{2j,k} & v_{2j+1,k} \end{bmatrix}, \quad (8)$$

where $V_j[0]$ represents the drop volume in the new area of interest before the k^{th} drop has been deposited at cell $(1, j)$; $V_j[1]$ represents the drop volume in the new area of interest after the k^{th} drop has been deposited at cell $(1, j)$.

The drop area coverage of the new area of interest centered at cell $(1, j)$ is given by

$$A_j[0] = \begin{bmatrix} a_{0j-1,k-1} & a_{0j,k-1} & 0 \\ a_{1j-1,k-1} & a_{1j,k-1} & 0 \\ a_{2j-1,k-1} & a_{2j,k-1} & 0 \end{bmatrix}, A_j[1] = \begin{bmatrix} a_{0j-1,k} & a_{0j,k} & a_{0j+1,k} \\ a_{1j-1,k} & a_{1j,k} & a_{1j+1,k} \\ a_{2j-1,k} & a_{2j,k} & a_{2j+1,k} \end{bmatrix}, \quad (9)$$

where $A_j[0]$ represents the drop area coverage in the new area of interest before the k^{th} drop has been deposited at cell $(1, j)$; $A_j[1]$ represents the drop area coverage in the new area of interest after the k^{th} drop has been deposited at cell $(1, j)$.

From Eq. (8) and (9), assuming a first drop has been deposited at cell $(1,1)$, the drop volume and area coverage in the new area of interest (3×3 area centered at cell $(1,2)$) before a second drop depositing at cell $(1,2)$ is

$$V_2[0] = \begin{bmatrix} v_{01,1} & v_{02,1} & 0 \\ v_{11,1} & v_{12,1} & 0 \\ v_{21,1} & v_{22,1} & 0 \end{bmatrix}, \quad \text{and} \quad A_2[0] = \begin{bmatrix} a_{01,1} & a_{02,1} & 0 \\ a_{11,1} & a_{12,1} & 0 \\ a_{21,1} & a_{22,1} & 0 \end{bmatrix} \quad (10)$$

where the first two columns of $V_2[0]$ and $A_2[0]$ are the second and third columns of $V_1[1]$ and $A_1[1]$, where

$$V_1[1] = \begin{bmatrix} v_{00,1} & v_{01,1} & v_{02,1} \\ v_{10,1} & v_{11,1} & v_{12,1} \\ v_{20,1} & v_{21,1} & v_{22,1} \end{bmatrix}, \quad \text{and} \quad A_1[1] = \begin{bmatrix} a_{00,1} & a_{01,1} & a_{02,1} \\ a_{10,1} & a_{11,1} & a_{12,1} \\ a_{20,1} & a_{21,1} & a_{22,1} \end{bmatrix}. \quad (11)$$

Using the above notation, a height profile propagation model can be written as

$$V_j[1] = V_j[0] + \Delta V \quad \text{and} \quad A_j[1] = A_j[0] + \Delta A, \quad (12)$$

where $\Delta V, \Delta A$ are cell volume change matrix and area coverage change matrix, respectively. Given the volume and area associated with the new area of interest, the height profile for the new area of interest is

$$H_j[1] = \frac{V_j[1]}{A_j[1]}, \quad (13)$$

where the division above is elemental division.

For the two drop example above, after the second drop has been deposited at cell (1,2), the height profile in the new area of interest is

$$H_2[1] = \begin{bmatrix} h_{01,2} & h_{02,2} & h_{03,2} \\ h_{11,2} & h_{12,2} & h_{13,2} \\ h_{21,2} & h_{22,2} & h_{23,2} \end{bmatrix} = \begin{bmatrix} v_{ij2} \\ a_{ij2} \end{bmatrix}, \quad (14)$$

where $i = 0, 1, 2$ and $j = 1, 2, 3$.

This section is further divided into 2 parts, with cell volume propagation model in Section 3.1 and area coverage propagation model in Section 3.2.

3.1 VOLUME PROPAGATION

Experimental data will be used to determine ΔV for the volume propagation model. The single drop volume is given by Eq. (4), i.e.

$$V = \begin{bmatrix} v_{00} & v_{01} & v_{02} \\ v_{00} & v_{11} & v_{12} \\ v_{00} & v_{21} & v_{22} \end{bmatrix} = V_1[1] = \begin{bmatrix} v_{00,1} & v_{01,1} & v_{02,1} \\ v_{10,1} & v_{11,1} & v_{12,1} \\ v_{20,1} & v_{21,1} & v_{22,1} \end{bmatrix}. \quad (15)$$

$V_2[0]$ can be written as

$$V_2[0] = \begin{bmatrix} v_{01,1} & v_{02,1} & 0 \\ v_{11,1} & v_{12,1} & 0 \\ v_{21,1} & v_{22,1} & 0 \end{bmatrix}. \quad (16)$$

The second drop is deposited at cell (1,2) after the drop at cell (1,1) is cured with UV light. After the second drop is cured, $V_2[1]$ can be obtained from experiment. ΔV can then be obtained by

$$\Delta V = V_2[1] - V_2[0], \quad \text{or} \quad \Delta V = [\Delta v_{ij}] = [v_{ij,2} - v_{ij,1}]. \quad (17)$$

3.2 AREA PROPAGATION

Area propagation follows the same approach as volume propagation, where the single drop area coverage is given by Eq. (2), i.e.

$$A = \begin{bmatrix} a_{00} & a_{01} & a_{02} \\ a_{00} & a_{11} & a_{12} \\ a_{00} & a_{21} & a_{22} \end{bmatrix} = A_1[1] = \begin{bmatrix} a_{00,1} & a_{01,1} & a_{02,1} \\ a_{10,1} & a_{11,1} & a_{12,1} \\ a_{20,1} & a_{21,1} & a_{22,1} \end{bmatrix}. \quad (18)$$

$A_2[0]$ can be written as

$$A_2[0] = \begin{bmatrix} a_{01,1} & a_{02,1} & 0 \\ a_{11,1} & a_{12,1} & 0 \\ a_{21,1} & a_{22,1} & 0 \end{bmatrix}. \quad (19)$$

The second drop is deposited at cell (1,2) after the drop at cell (1,1) is cured with UV light. After the second drop is cured, $A_2[1]$ can be obtained from measurement. ΔA can then be obtained by

$$\Delta A = A_2[1] - A_2[0], \quad \text{or} \quad \Delta A = [\Delta a_{ij}] = [a_{ij,2} - a_{ij,1}]. \quad (20)$$

4 EXPERIMENTAL VALIDATION

Experiments are carried out to validate the propagation model. We calculate ΔV and ΔA from 2-drop experiments. Then we use them to predict the height profile from a 3-drop line ($H_3[1]$). Analysis is based on RMS error, which can be calculated by

$$RMS = \sqrt{\frac{1}{N} \left(\frac{V_p - V_m}{V_m} \right)^2}, \quad (21)$$

where N is number of samples; V_p and V_m are predicted and measured values, respectively.

To obtain enough data, we print and analyze 50 samples of single-drop, 2-drop and 3-drop pattern each, at 70 μm pitch. Single-drop data is shown in Section 2.

4.1 CALCULATE ΔV AND ΔA

To avoid coalescence, the first drop is cured under UV light for 1.5 seconds, before the second drop is deposited. This longer

TABLE 4. Measured and predicted cell volume (μm^3) in each cell of 2 drops.

442.99 (474.52)	5277.37 (5875.85)	6719.44 (6962.56)	1385.46 (1444.70)
5955.36 (6105.06)	32180.14 (32162.25)	35927.41 (35830.02)	10632.84 (10128.87)
467.12 (4779.55)	5350.54 (6042.79)	7301.58 (6927.05)	1343.83 (1406.72)

TABLE 5. Measured and predicted area coverage (μm^2) in each cell of 2 drops.

312.36 (340.04)	1908.15 (1981.17)	2176.14 (2039.23)	549.70 (557.95)
1946.35 (1923.37)	4984.03 (4961.9)	4984.03 (4961.9)	3013.14 (2862.69)
314.83 (338.93)	1965.58 (2011.72)	2007.68 (2078.33)	556.97 (543.01)

TABLE 6. Calculated ΔV

395.75	6472.00	1444.70
634.93	29698.74	10128.87
396.59	6442.31	1406.72

time is setup to capture dynamics of each additional drop. The printing orders can be adjusted, such that all non-adjacent drops can be printed and cured at once. As a result, large format printing would not take a long time. With 50 samples in total, we randomly separate 2-drop samples to 3 groups of 15 samples and 1 group of 5 samples. Two groups of 15 samples are used to obtain $V_2[1]$ and $A_2[1]$. Then $V_2[1]$ and $A_2[1]$ are compared with samples in the other groups, to confirm consistency of results.

2-drop measurements are shown in Table 4, 5 and 8, with predicted values in bold. The cell volume change matrix (ΔV) and the area coverage change matrix (ΔA) can be obtained from Eq. (17) and (20), shown in Table 6 and 7, respectively. Two values of ΔA are not calculated, because the two cells will always be fully filled. Values are larger in cells without prior ink, which is as expected.

4.2 RESULTS OF 3-DROP PATTERN

After obtaining ΔV and ΔA , it is possible to check how well does the propagation model predict height profiles of 3 consec-

TABLE 7. Calculated ΔA

39.10	1705.13	557.95
N/A	N/A	2862.69
51.52	1744.58	543.01

TABLE 8. Measured and predicted height (μm) in each cell of 2 drops.

1.42 (1.40)	2.77 (2.97)	3.09 (3.41)	2.52 (2.59)
3.06 (3.17)	6.46 (6.48)	7.21 (7.22)	3.53 (3.54)
1.48 (1.41)	2.72 (3.00)	3.64 (3.33)	2.41 (2.59)

TABLE 9. Measured and predicted volume (μm^3) in each cell of 3 drops.

572.0 (443.0)	6033.9 (5277.4)	7411.2 (7115.2)	7183.1 (7857.5)	1948.9 (1444.7)
6920.21 (5955.4)	31280.0 (32180.1)	36622.8 (36562.3)	36940.6 (40331.58)	15521.6 (10128.8)
686.26 (467.1)	6673.4 (5350.5)	7270.7 (7698.2)	6361.44 (7786.1)	1904.9 (1406.7)

TABLE 10. Measured and predicted area (μm^2) in each cell of 3 drops.

459.9 (312.4)	2325.3 (1908.2)	2491.0 (2215.2)	2424.3 (2254.8)	833.4 (557.9)
2288.3 (1946.4)	4956.2 (4984.0)	4952.4 (4984.0)	4938.8 (4984.0)	3902.1 (2862.7)
448.6 (314.8)	2317.7 (1965.6)	1955.5 (2059.2)	1844.0 (2301.5)	776.6 (543.0)

utive drops. So we use Eq. (12) to predict $V_3[1]$ and $A_3[1]$ before obtaining predicted $H_3[1]$ with Eq. (13). Table 9, 10 and 11 show measured cell volume, area coverage and cell height in each cell, with predicted values in bold, respectively. Error analysis is based on RMS errors, which can be calculated with Eq. (21).

Figure 4.(a) is the height contour of one of the 3-drop sam-

TABLE 11. Measured and predicted height (μm) in each cell of 3 drops.

1.24 (1.42)	2.59 (2.77)	2.98 (3.21)	2.96 (3.48)	2.34 (2.59)
3.02 (3.06)	6.31 (6.46)	7.39 (7.34)	7.48 (8.09)	3.98 (3.54)
1.53 (1.48)	2.66 (2.72)	3.72 (3.74)	3.45 (3.38)	2.45 (2.59)

TABLE 12. RMS error comparison among 3 models

	Superposition	Graph-based	This Model
RMS Error	14.2%	17.2%	7.4%

TABLE 13. Max cell height of 3-drop, 4-drop and 5-drop printing.

Number of Drops	3	4	5
Max Cell Height (μm)	7.48	8.19	8.02

with 7.4% among all cells. Table 12 shows the comparison of modeling RMS error among 3 height models. Both graph-based dynamic model and superposition model are above 10%.

4.3 HEIGHT PROFILE STABILITY TEST

3-drop prediction confirms that our proposed model works better than existing models. Cell height along center row shows an upward trend, which raises concern on stability. From common sense, we know that printing a line will not lead to monotonically increasing cell height along center row. The predicted maximum cell height at center row can be calculated by

$$h_{\max} = \frac{\sum_{j=0}^2 \Delta v_{1j}}{a_{11}} = 8.15 \mu m. \quad (22)$$

Besides theoretical calculation, experimental results also confirm the stability of height profiles. Table 13 shows the peak cell height from 3-drop, 4-drop and 5-drop printings. The maximum deviation from predicted max cell height is 8.2%.

5 CONCLUSION

In this paper, we proposed a height profile propagation model for drop-on-demand printing of UV curable inks. The model uses one and two drop height profiles to predict the height profiles of subsequent drops. The fundamental idea is based on material flow due to substrate height difference. 3-drop height profile prediction is validated with experiments. RMS error along center row is 6.2% and that of all cells is 7.4%, both of which are better than existing models. Additional work is needed to analyze the stability of the proposed propagation model as well as additional experimental validation are needed.

REFERENCES

- [1] A. Ufuk Agar and Jan P. Allebach. Model-based color halftoning using direct binary search. *IEEE Transactions on Image Processing*, 14(12):1945–1959, 2005.

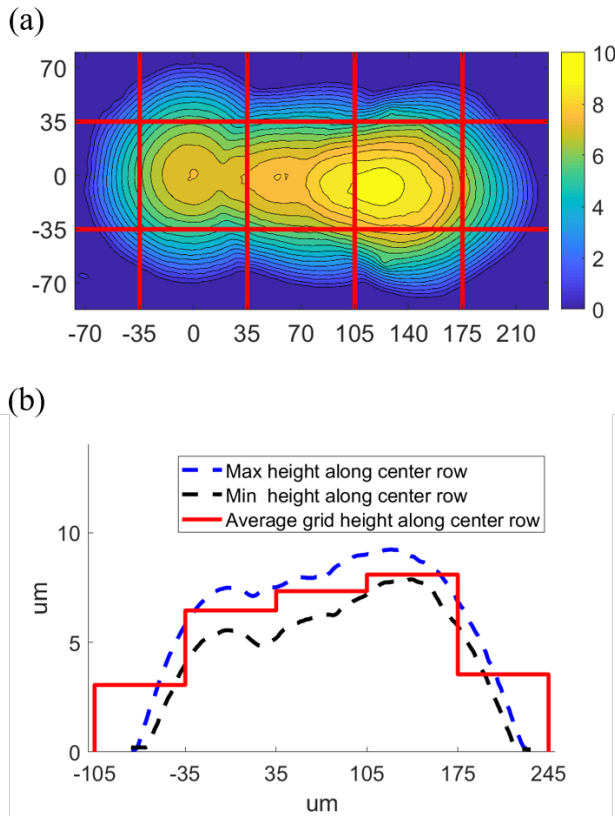


FIGURE 4. (a): Contour of 3 drops, marked with $70 \mu m$ pitch size. (b): Dash lines are height measurements of the sample in a), with blue dash line showing the maximum height along the center row and black dash line showing the minimum height along the center row; red solid line shows the average cell height long center row.

ples, with red solid line marking the boundaries of each cell. Figure 4.(b) shows the maximum and minimum height of each column measured along center row, and predicted height profile. It can be observed that the predicted height match the trend of actual measurements. RMS error is 6.6% along the center row,

- [2] ASTM International. ISO/ASTM52900-15 standard terminology for additive manufacturing – general principles – terminology. *ASTM International*, 2015.
- [3] Moonhyeok Choi, Gihun Son, and Woosup Shim. Numerical simulation of droplet impact and evaporation on a porous surface. *International Communications in Heat and Mass Transfer*, 80:18–29, 2017.
- [4] Patrick Cooley, David Wallace, and Bogdan Antohe. Applications of ink-jet printing technology to biomems and microfluidic systems. *JALA: Journal of the Association for Laboratory Automation*, 7(5):33–39, 2002.
- [5] Charalabos Doumanidis and Eleni Skordeli. Distributed-Parameter Modeling for Geometry Control of Manufacturing Processes With Material Deposition. *Journal of Dynamic Systems, Measurement, and Control*, 122(1):71, 2000.
- [6] Simon Ford and Mélanie Despeisse. Additive manufacturing and sustainability: an exploratory study of the advantages and challenges. *Journal of Cleaner Production*, 137:1573–1587, 2016.
- [7] PR Gunjal, VV Ranade, and RV Chaudhari. Experimental and computational study of liquid drop over flat and spherical surfaces. *Catalysis today*, 79:267–273, 2003.
- [8] Yijie Guo, Joost Peters, Tom Oomen, and Sandipan Mishra. Control-oriented models for ink-jet 3D printing. *Mechatronics*, 56:211–219, 2018.
- [9] Hue P Le. Progress and trends in ink-jet printing technology. *Journal of Imaging Science and Technology*, 42(1):49–62, 1998.
- [10] Pingshan Li and Jan P. Allebach. Tone-dependent error diffusion. *IEEE Transactions on Image Processing*, 13(2):201–215, 2004.
- [11] Henning Siringhaus and Tatsuya Shimoda. Inkjet printing of functional materials. *MRS bulletin*, 28(11):802–806, 2003.